Research Square

Preprints are preliminary reports that have not undergone peer review.
They should not be considered conclusive, used to inform clinical practice,
or referenced by the media as validated information.

Glyphosate disrupts spermatogonial cell-cycle progression via reduced Sertoli cell-derived lactate availability

Yu-Long Ren
Shandong Agricultural University
Qing Liang
Shandong Agricultural University
Kai Chen
Shandong Academy of Pharmaceutical Sciences
Yan-Zhan Jia
Shandong Agricultural University
Hao Wang
Shandong Agricultural University
Lin Wang
wanglin2013@sdau.edu.cn
Shandong Agricultural University

Research Article

Keywords: Glyphosate, Sertoli cells, Lactate, Spermatogonia, Cell cycle, SUMOylation

Posted Date: November 18th, 2026

DOI: https://doi.org/10.21203/rs.3.rs-11589535/v1

License: This work is licensed under a Creative Commons Attribution 4.0 International License.
Read Full License

Additional Declarations: No competing interests reported.

Glyphosate disrupts spermatogonial cell-cycle progression via reduced Sertoli cell-derived lactate availability

Yu-Long Ren [a, b,1], Qing Liang [a,1], Kai Chen [c], Yan-Zhan Jia [a], Hao Wang [a], Lin Wang [a*]

a College of Veterinary Medicine, Shandong Provincial Key Laboratory of Zoonoses, Shandong Agricultural University, 7 Panhe Street, Tai'an, Shandong 271017, China.

b College of Animal Science, Heilongjiang Bayi Agricultural University, Daqing, Heilongjiang 163319, China.

c Shandong Center of Technology Innovation for Engineered Bacteriophage Therapeutics, Shandong Academy of Pharmaceutical Sciences, Ji'nan, Shandong 250101, China.

[1] These authors contributed equally.

Corresponding author: Prof. Dr. Lin Wang

Tel: +86-538-8242478; Fax: +86 538-8241419

E-mail address: wanglin2013@sdau.edu.cn (Wang L)

Abstract

Glyphosate (GLY), a widely used herbicide, has raised increasing concern regarding male reproductive toxicity. Lactate produced by Sertoli cells provides essential metabolic support for developing germ cells; however, whether GLY-induced disruption of this support affects spermatogonial cell-cycle progression remains unclear. Here, we combined a chronic dietary GLY exposure mouse model with a Transwell co-culture system of mouse Sertoli cells (TM4) and spermatogonial cells (GC-1). GLY exposure reduced testicular spermatogonial numbers and impaired sperm quality. In co-culture, GLY-treated TM4 cells decreased lactate availability and induced G2/M accumulation in GC-1 cells, accompanied by altered expression of cell-cycle regulators. Pharmacological inhibition of lactate transport (AZD0095) similarly increased the G2/M fraction, whereas lactate supplementation attenuated G2/M accumulation in co-cultures containing GLY-treated TM4 cells. Mechanistically, reduced lactate availability was associated with increased SENP1 (SUMO-specific protease 1) expression and decreased SUMO2/3 modification of APC4 (anaphase-promoting complex subunit 4) in GC-1 cells. SENP1 knockdown restored APC4 SUMO2/3 modification and alleviated G2/M accumulation. Moreover, the APC4 K772R/K797R double mutation weakened the effects of lactate supplementation on Cyclin B1 and CDK1 expression and on G2/M progression. In summary, GLY-induced reduction of Sertoli cell-derived lactate disrupts spermatogonial cell-cycle progression via SENP1-mediated APC4 deSUMOylation. These findings reveal a novel metabolic mechanism underlying GLY male reproductive toxicity.

Keywords: Glyphosate; Sertoli cells; Lactate; Spermatogonia; Cell cycle; SUMOylation

1. Introduction

Male reproductive health has become an increasing public health concern worldwide, with declining semen quality and reduced fertility reported in recent decades(Pallotti et al. 2025). In addition to genetic and lifestyle factors, exposure to environmental chemicals is considered an important contributor to male reproductive dysfunction(Edenfield et al. 2025). Glyphosate (GLY) is a broad-spectrum herbicide widely used in agriculture, and its extensive, long-term application has led to GLY residues in soil(Ferreira et al. 2023), water(Schwientek et al. 2024), and agricultural products(Rampazzo et al. 2023; Souza et al. 2023), raising concerns about its potential health effects. Given its potential endocrine-disrupting activity, the adverse effects of GLY on the male reproductive system have received increasing attention. Previous studies have reported that exposure to GLY can damage Sertoli cells, disrupt blood–testis barrier integrity (Liu et al. 2022), and impair sperm quality(Yang et al. 2022; Ren et al. 2026). However, how GLY-induced Sertoli cell dysfunction affects germ cell development and spermatogenesis remains poorly understood.

Lactate is a major glycolytic metabolite produced and secreted by Sertoli cells(Rato et al. 2012; Ni et al. 2019). Although traditionally regarded primarily as a metabolic waste product, lactate is now recognized as both an energy substrate and a signaling molecule involved in diverse biological processes (Li et al. 2022; Dai and Wei 2023). Within the testis, developing germ cells preferentially utilize Sertoli cell-derived lactate to meet the metabolic demands of their growth and developmental progression (Estermann et al. 2026a). Spermatogonial proliferation is an early event in spermatogenesis that maintains the spermatogonial pool and supplies cells for subsequent stages of germ cell development(Staub and Johnson 2018). This

process requires sustained metabolic support for biosynthesis and cell-cycle progression (Griswold 2016; Li et al. 2024). Because lactate serves both as a carbon source for biosynthesis and as a metabolic signal, reduced Sertoli cell-derived lactate availability may compromise the metabolic support required for normal spermatogonial cell-cycle progression. Our previous study showed that chronic dietary GLY exposure disrupts glycolytic metabolism in Sertoli cells and reduces testicular lactate levels(Ren et al. 2025a). However, whether this reduction contributes to GLY-induced spermatogonial cell-cycle disturbances has not been established.

Cell-cycle progression depends on the coordinated activity of cyclins, cyclin-dependent kinases, and protein degradation pathways(Gupta and Chaudhuri 2022). The anaphase-promoting complex/cyclosome (APC/C) is a central E3 ubiquitin ligase complex that governs mitotic progression and exit by targeting key cell-cycle regulators for degradation(Vodermaier 2004; Chang et al. 2015). APC4 is a core subunit of APC/C and contributes to the structural integrity and functional activity of the complex(Eifler et al. 2018). Small ubiquitin-like modifier (SUMO)ylation provides an additional layer of post-translational regulation, influencing protein stability, localization, interactions, and activity(Eifler and Vertegaal 2015a)(Bellail et al. 2014; Kroonen and Vertegaal 2021). The balance of SUMOylation is maintained by SUMO-conjugating enzymes and Sentrin/SUMO-specific proteases (SENPs), which remove SUMO modifications from target proteins(Claessens and Vertegaal 2024). Although SUMOylation has been implicated in cell-cycle regulation, whether APC4 SUMOylation contributes to lactate-dependent regulation of spermatogonial cell-cycle progression remains unknown.

In this study, a mouse model of chronic dietary GLY exposure and a TM4/GC-1 Transwell co-culture system were used to investigate how GLY-induced reductions in Sertoli cell-derived lactate availability affect spermatogonial cell-cycle progression and to elucidate the molecular mechanisms underlying GLY-induced male reproductive toxicity.

2. Materials and methods

2.1 Animal experimental design

All experimental procedures were approved by the Shandong Agricultural University Animal Care and Use Committee (SDAUA-2024-022). Forty-five healthy 6-week-old male C57BL/6 mice were purchased from Pengyue Laboratory Animal Breeding Co., Ltd. (Jinan, China). The mice were housed under specific pathogen-free (SPF) conditions at 22 ± 2℃ and 58 ± 8% relative humidity with a 12 h light/dark cycle. After 1 week of acclimation to a standard diet, the mice were randomly divided into three groups (n = 15 per group): control group (receiving a normal diet), L-GLY group (receiving 8.75 mg GLY/kg diet), and H-GLY group (receiving 87.5 mg GLY/kg diet). GLY used for in *vivo* studies (No. 337757) and in *vitro* studies (No. 90479) was purchased from Sigma-Aldrich (St. Louis, MO, USA). The L-GLY doses were based on the human acceptable daily intake (ADI) of 1.75 mg/kg body weight/day established by the U.S. Environmental Protection Agency, and it is comparable to reported GLY residue levels in soybeans(Bøhn and Millstone 2019). The H-GLY dose, corresponding to 17.5 mg/kg body weight/day, was below the no-observed-adverse-effect level (NOAEL, 50 mg/kg body weight/day) for mice. During the experiment, mice had free access to food and water, and body weight and food intake were recorded weekly. After 24 weeks of exposure, testes, epididymal tissues, and sperm were collected for subsequent

analyses.

2.2 Computer-Assisted Sperm Analysis (CASAs)

The dissected epididymis was incubated in M199 medium (M9163, MedChemExpress, USA) at 37℃ for 10 min to facilitate sperm release. The resulting suspension was collected by transferring the medium into a centrifuge tube. Sperm concentration, motility, progressive, rapid, slow, and static percentages were analyzed using a computer-assisted sperm analyzer (Hamilton, TOX IVOS, USA). Representative images were also acquired for further evaluation.

2.3 Histological Analysis

Testes and epididymal tissues were fixed in 4% paraformaldehyde (G1101, Servicebio, China) for 48 h, dehydrated through graded ethanol (70%, 80%, 90%, 95%, and 100%), and embedded in paraffin. Sections of 5 μm thickness were prepared from the embedded tissues. Following deparaffinization and rehydration, the sections underwent hematoxylin-eosin (H&E) staining and were examined under a light microscope to evaluate the morphology of spermatogenic tubules. Quantification of spermatogonia, primary spermatocytes, and spermatids was performed using ImageJ software (v1.8.0). Fifteen seminiferous tubules were randomly selected from each testis, representing approximately 10% of the total testicular area.

2.4 Western blotting Analysis

Western blotting was conducted following our established protocol(Ren et al. 2024). Briefly, cells or tissues were homogenized in RIPA buffer (WB3100, New Cell Molecular Biotech, China), combined with sample buffer (PN2252, G-GLONE, China), and denatured at 100℃ for 5 min. Proteins were separated by sodium dodecyl sulfate-polyacrylamide gel

electrophoresis (SDS−PAGE), transferred to polyvinylidene difluoride membranes (PVDF, Millipore, USA). The membranes were incubated with 5% skim milk for 90 min to block nonspecific binding, then probed with primary antibodies at 4℃ overnight and secondary antibodies at room temperature for 50 min. Antibody information is provided in Table S1. Target proteins were detected using ChemiDoc XRS (Bio-Rad, Marnes-LaCoquette, France) and quantified via grayscale analysis using ImageJ software (v1.8.0).

2.5 Transcriptome sequencing and analysis

Total RNA extraction from mouse testes was performed with TRIzol reagent (Vazyme Biotech Co., Ltd., Nanjing, China). Strand-specific libraries were constructed with the NEBNext Ultra II RNA Library Prep Kit (New England Biolabs Inc., Ipswich, MA, USA), and library quality was evaluated on an Agilent 2100 Bioanalyzer (Agilent Technologies Inc., CA, USA). Libraries were sequenced on an Illumina platform in PE150 mode. Differentially expressed genes (DEGs) analysis was performed with DESeq (v1.38.3) to identify DEGs with $|\log2FoldChange| > 1$ and $p < 0.05$. Functional annotation was achieved through GO enrichment analysis using topGO (v2.50.0) ($p < 0.05$).

2.6 Lactate level measurement

Following the manufacturer's protocol, the lactate levels in testicular tissues and the medium collected from the lower chamber of Transwell plates were quantified using a lactate assay kit (BC2235, Solarbio, China). The specific operational steps refer to previous research(Ren et al. 2025b).

2.7 Transwell Co-culture Experimental Protocol

The Transwell system was used to investigate the effect of lactate secreted by Sertoli cells

(TM4 cells, CRL-1715, ATCC, Manassas, VA) on the proliferation of Spermatogonium (GC-1 cells, CRL-2053, ATCC, Manassas, VA), following the detailed steps for cell co-culture according to previous reports(Justus et al. 2023). GC-1 cells were plated in the lower chamber of a 6-well Transwell plate at a density of 3×10^5 cells per well and incubated at 37℃ with 5% CO_2 for 3 h to ensure complete adhesion. TM-4 cells were pretreated with AZD0095 (an MCT4 inhibitor, HY-148517, MedChemExpress, USA) or GLY for 24 h, then resuspended in fresh DMEM/F12 medium (PM150312, Procell, China). A total of 2 mL cell suspension (containing 1×10^5 cells) was gently added to the upper chamber of the Transwell system. The assembled Transwell system was maintained under standard culture conditions (37℃, 5% CO_2) to investigate time-dependent effects of TM4-derived lactate on GC-1 cell responses. For lactate supplementation, the medium containing 10 mM lactic acid sodium (LAS, 71718, MedChemExpress, USA) was replaced in the lower chamber after the complete adhesion of GC-1 cells.

2.8 Cell cycle analysis

GC-1 cells were cultured to approximately 40% confluence and synchronized using a double thymidine block. Briefly, cells were treated with 2 mM thymidine for 18 h, released in fresh DMEM/F12 for 9 h, and then treated again with 2 mM thymidine for another 18 h. After synchronization, cells were washed with PBS and released in regular DMEM/F12. Cells were collected at 0, 8, 16, 24, 32, 40, and 48 h after release to assess cell-cycle progression, and 48 h was selected for subsequent drug-treatment experiments. Cell-cycle distribution was analyzed using a cell cycle detection kit (AC101, Vazyme Biotech Co., Ltd., Nanjing, China). Cells were stained with propidium iodide/RNase A solution, incubated at 37℃ for 40 min in

the dark, and analyzed using an Attune NxT flow cytometer (Thermo Fisher Scientific, China). DNA content and cell-cycle distribution were quantified using FlowJo software version 10.8.1.

2.9 Measurement of nuclear diameter and volume

After the indicated treatments, GC-1 cells grown on round coverslips in the lower chambers of Transwell plates were fixed with 4% paraformaldehyde for 8 min, washed with PBS, and permeabilized with 0.1% Triton X-100 at room temperature for 12 min. After washing, the coverslips were mounted with DAPI-containing antifade mounting medium (P0131, Beyotime, China) and sealed with clear nail polish. Images were captured using a confocal microscope. Nuclear diameter was measured using Imaris Viewer software version 10.2, and nuclear volume was calculated using the formula $V = 4/3\pi r^3$, where r represents the nuclear radius(Foy et al. 2023).

2.10 siRNA transfection

Three siRNAs targeting mouse SENP1 and a negative control siRNA were synthesized by Sigma-Aldrich (Shanghai, China). The sequences were shown in Table S2. GC-1 cells were seeded in 6-well plates and transfected with si-SENP1 or si-NC at a final concentration of 20 nM using Lipofectamine® RNAiMAX in Opti-MEM. After 6 h of transfection, the medium was replaced with fresh complete medium, and the cells were further cultured until they reached approximately 70% confluence. SENP1 knockdown efficiency was evaluated by western blotting, and the most effective siRNA was selected for subsequent experiments.

2.11 Construction of the APC4-K772R/K797R double-mutant plasmid

The APC4 SUMOylation-site mutant plasmid was constructed by Wuhan Miaoling Biotechnology Co., Ltd. (Wuhan, China). Briefly, APC4 was amplified by PCR and inserted

into the pCMV-T7-MCS-3×FLAG-WPRE-Neo expression vector through homologous recombination. To generate a SUMOylation-deficient APC4 mutant, lysine residues at positions 772 and 797 were simultaneously substituted with arginine residues, resulting in the double-mutant expression plasmid APC4-K772R/K797R(Day et al. 2024). The recombinant products were transformed into DH5α competent cells, and positive clones were selected by antibiotic screening and colony PCR. Plasmids were then extracted from positive clones, and the inserted sequence and mutation sites were confirmed by DNA sequencing.

2.12 Immunoprecipitation analysis of APC4 SUMO2/3 modification

Treated cells were lysed in RIPA buffer supplemented with protease inhibitors and N-ethylmaleimide (NEM, HY-D0843, MedChemExpress, USA). After centrifugation, equal amounts of total protein were incubated with an anti-APC4 antibody or isotype IgG control overnight at 4℃, followed by incubation with Protein A/G agarose beads for 4 h at 4℃. The immunoprecipitates were washed, denatured in protein loading buffer, separated by SDS-PAGE, and transferred onto PVDF membranes. After blocking, the membranes were incubated with an anti-SUMO2/3 primary antibody overnight at 4℃ and then with an HRP-conjugated secondary antibody. Protein signals were visualized using an ECL detection system, and APC4 SUMO2/3 modification was evaluated based on the SUMO2/3 signal detected in APC4 immunoprecipitates.

2.13 Statistical analysis

All experiments were performed with at least three independent biological replicates. Data are presented as the mean ± SEM. For relative quantification, data were normalized to the corresponding control group and expressed as fold change. Statistical analyses were performed

using IBM SPSS Statistics 23.0. Student's t-test was used for comparisons between two groups, and one-way ANOVA followed by Tukey's post hoc test was used for multiple-group comparisons. Spearman's rank correlation analysis was used to evaluate correlations between variables, and linear regression analysis was used to assess the relationship between lactate levels and spermatogonia populations in the testis. Graphs were generated using GraphPad Prism 7. Statistical significance was defined as * $p < 0.05$, ** $p < 0.01$.

3. Results

3.1 GLY exposure reduces spermatogonial numbers and impairs sperm quality in mice

The experimental design is shown in Fig. 1A. Compared with the control group, sperm concentration and motility were significantly reduced in both GLY-exposed groups (Fig. 1B). Histological examination of the epididymis revealed markedly reduced sperm content in the lumens of both the caput and cauda epididymides in the GLY-exposed groups compared with the control group (Fig. 1C). Testicular histology showed reduced numbers of spermatogenic cells at different stages within the seminiferous tubules in both GLY-exposed groups (Fig. 1D). In addition, the testicular coefficient was significantly lower in the H-GLY group, whereas the epididymal coefficient did not differ significantly among the three groups (Fig. 1E). Quantitative analysis further showed that the number of spermatogonia per seminiferous tubule was significantly lower in both GLY-exposed groups than in the control group (Fig. 1F).

3.2 GLY-induced changes in lactate availability are associated with cell-cycle-related changes in GC-1 cells

To investigate the reduction in spermatogonia observed in GLY-exposed mice, a Transwell

co-culture system comprising TM4 and GC-1 cells was established. The results of cell cycle-related protein expression in GC-1 cells are shown in Fig. 2A. In the control co-culture system, Cyclin D1 and CDK4 protein levels peaked at 16 h and 24 h, respectively. Cyclin B1, CDK6, CDK1, and CDK2 reached their highest levels at 32 h, 16 h, 32 h, and 32 h, respectively. In the co-culture system containing GLY-treated TM4 cells, the peak levels of Cyclin D1, Cyclin B1, CDK4, CDK6, CDK1, and CDK2 occurred at 40 h, 48 h, 32 h, 40 h, 48 h, and 48 h, respectively. GC-1 cell nuclear diameter and cell volume were further assessed under the two co-culture conditions. The measured nuclear diameters were generally larger in GC-1 cells co-cultured with GLY-treated TM4 cells than in those co-cultured with untreated TM4 cells. Quantitative analysis also showed a significant increase in GC-1 cell volume in the GLY-treated TM4 co-culture group (Fig. 2B). Extracellular lactate levels in TM4 cell cultures increased progressively during the 48 h culture period, reaching 8.47 ± 0.693 mmol/L at 48 h (Fig. 2C). In contrast, GLY reduced extracellular lactate levels in a concentration-dependent manner, with lower levels observed at increasing GLY concentrations (Fig. 2D). Intracellular lactate levels in GC-1 cells co-cultured with untreated TM4 cells increased from 2.214 ± 0.080 mmol/gprot at 0 h to 8.285 ± 0.242 mmol/gprot at 32 h, followed by a decrease at 40 and 48 h. In contrast, intracellular lactate levels increased more gradually in GC-1 cells co-cultured with GLY-treated TM4 cells, reaching 6.190 ± 0.178 mmol/gprot at 48 h. The peak in intracellular lactate levels at 32 h in the control co-culture system coincided with the peak expression of Cyclin B1 and CDK1, whereas both lactate levels and the expression of these proteins peaked at later time points in the GLY-treated TM4 co-culture system (Fig. 2E). Regression analysis further revealed a positive correlation between lactate levels and

spermatogonial numbers ($R^2 = 0.921$, Fig. 2F).

3.3 Lactate availability modulates GLY-induced cell-cycle alterations in GC-1 cells

To further examine the effects of lactate availability on GC-1 cell-cycle progression, AZD0095 was used to inhibit lactate transport, followed by analysis of Cyclin B1 and CDK1 expression and cell-cycle distribution. As shown in Fig. 3A, AZD0095 reduced extracellular lactate levels in TM4 cells in a dose-dependent manner. GLY and AZD0095 treatments increased Cyclin B1 and CDK1 protein levels in GC-1 cells, whereas LAS supplementation reduced the GLY-associated increases in both proteins (Fig. 3B). GC-1 cells cultured with LAS alone also showed lower Cyclin B1 and CDK1 levels than those cultured with NaCl alone. Flow cytometric analysis showed that both GLY and AZD0095 treatment reduced the proportion of GC-1 cells in the G0/G1 phase and increased the proportion in the G2/M phase. LAS supplementation attenuated these changes in the GLY-treated group (Fig. 3C). Consistently, both GLY and AZD0095 increased GC-1 cell nuclear diameter and volume, whereas LAS supplementation reversed GLY-induced nuclear enlargement (Fig. 3D).

3.4 SENP1 contributes to GLY-induced G2/M-phase accumulation associated with reduced lactate availability

Venn analysis of genes associated with germ cell development, male germ cell proliferation, regulation of male germ cell proliferation, and the mitotic cell cycle identified SENP1 as the only overlapping gene. SENP1 mRNA and protein levels were significantly elevated in the testes of GLY-exposed mice compared with the control group (Fig. 4A, B). In the Transwell co-culture system, GLY treatment of TM4 cells and AZD0095 treatment significantly increased SENP1 protein levels in GC-1 cells. LAS supplementation significantly reduced

SENP1 protein levels in the GLY-treated TM4 co-culture group. SENP1 protein levels were also significantly lower in the GC-1 + LAS group than in the GC-1 + NaCl group (Fig. 4C). In GC-1 cells co-cultured with GLY-treated TM4 cells, SENP1 knockdown significantly reduced Cyclin B1 and CDK1 protein levels compared with the NC + GLY group (Fig. 4D). Flow cytometric analysis showed that co-culture with GLY-treated TM4 cells significantly decreased the proportion of GC-1 cells in the G0/G1 phase and increased the proportion in the G2/M phase. SENP1 knockdown significantly reduced the G2/M-phase proportion in the GLY-treated TM4 co-culture group (Fig. 4E). Morphological assessment revealed larger nuclei in GLY-treated GC-1 cells, accompanied by an increase in cell volume. Both measurements were lower in the si-SENP1 + GLY group than in the NC + GLY group (Fig. 4F).

3.5 SENP1-dependent APC4 SUMOylation mediates lactate regulation of GLY-induced G2/M-phase accumulation

Given the deSUMOylase activity of SENP1, APC4 was examined as a potential downstream target of SENP1. Total APC4 protein levels did not differ significantly between the control and GLY groups, whereas APC4 SUMO2/3 modification was reduced in the GLY group (Fig. 5A, B). SENP1 knockdown increased APC4 SUMO2/3 modification in GC-1 cells co-cultured with GLY-treated TM4 cells compared with the corresponding NC + GLY group (Fig. 5C). To examine the contribution of APC4 SUMOylation to lactate-associated cell-cycle changes, an APC4 double mutant carrying K772R and K797R substitutions was generated (Fig. 5D). Immunoprecipitation followed by immunoblotting showed that LAS supplementation increased APC4 SUMO2/3 modification in cells expressing wild-type APC4. In contrast, APC4 SUMO2/3 modification was undetectable in cells expressing the

K772R/K797R mutant, regardless of LAS treatment (Fig. 5E). In cells expressing wild-type APC4, LAS supplementation reduced Cyclin B1 and CDK1 protein levels. These changes were not evident in cells expressing the K772R/K797R mutant (Fig. 5F). Flow cytometric analysis further showed that LAS supplementation reduced the proportion of G2/M-phase cells in the wild-type group. However, the G2/M-phase proportion did not differ significantly between the K772R/K797R and K772R/K797R + LAS groups (Fig. 5G, H). Furthermore, LAS supplementation did not significantly alter GC-1 cell volume in the WT group, whereas cell volume remained elevated in cells expressing the K772R/K797R mutant, with no significant difference between the mutant groups with and without LAS supplementation (Fig. 5I, J).

4. Discussion

Glyphosate (GLY) exposure has been increasingly associated with male reproductive dysfunction, and previous studies have shown that GLY can interfere with multiple processes involved in spermatogenesis(Lombó et al. 2025a, b; Maddalon et al. 2025). However, the metabolic mechanisms underlying GLY-induced germ-cell dysfunction remain poorly understood. In the present study, GLY exposure impaired sperm quality and testicular histology, accompanied by a reduction in spermatogonial numbers and lactate levels in the testes. In vitro experiments further showed that GLY treatment of Sertoli cells reduced lactate availability in the co-culture system and altered cell-cycle progression in GC-1 spermatogonial cells. Mechanistic analyses further implicated SENP1-associated APC4 deSUMOylation in these changes. These findings provide evidence linking altered lactate availability to GLY-associated disruption of spermatogonial cell-cycle progression and identify SENP1 and APC4

SUMOylation as potential components of this process.

Spermatogenesis is a metabolically demanding process that depends on the coordinated development of germ cells within a specialized testicular microenvironment(Maroto et al. 2025). Sertoli cells provide lactate as an energy substrate to support germ cell proliferation and differentiation(Feng et al. 2025). Although lactate was traditionally regarded as a metabolic end product of glycolysis, it is now recognized as an important fuel utilized by various cell types(Chen et al. 2025). Previous studies have shown that environmental toxicants, including nonylphenol, TiO_2 nanoparticles, and aflatoxin B1, can disrupt lactate production in Sertoli cells, highlighting the susceptibility of Sertoli cell lactate metabolism to toxicant exposure(Jiang et al. 2022; Han et al. 2023; Dong et al. 2024). Consistent with these findings, a previous study showed that chronic GLY exposure disrupted Sertoli cell glycolysis and reduced testicular lactate levels(Ren et al. 2025b). 29. However, the consequences of altered lactate availability for germ cell development remain poorly understood. A recent study demonstrated that in *vivo* blockade of lactate transport between Sertoli cells and germ cells led to germ cell loss under conditions of glycogen depletion(Estermann et al. 2026b). Given the metabolic support provided by Sertoli cell-derived lactate, reduced lactate availability may compromise the metabolic environment required for germ cell development and spermatogenic progression(Griswold 2016). In the present study, testicular lactate levels were strongly positively correlated with spermatogonial numbers ($R^2 > 0.89$). This finding further supports an association between testicular lactate levels and spermatogonial abundance.

Lactate serves not only as an energy substrate but also as a metabolic signal to coordinate cell cycle progression(Cluntun and Rutter 2023). Beyond ATP production, lactate has been

352 implicated in NAD^+ homeostasis, epigenetic regulation, and cell-cycle-related signaling
353 pathways(Li et al. 2022). Glycolysis is a major source of lactate, and its activity often increases
354 in proliferating cells to meet the metabolic demands of cell division(Liu et al. 2023). Previous
355 studies have also linked lactate accumulation to the timing of mitotic progression(Chen et al.
356 2023; Liu et al. 2023). Thus, lactate levels may reflect not only glycolytic activity but also the
357 metabolic state associated with cell-cycle progression. In the present study, reduced lactate
358 availability was accompanied by delayed expression peaks of Cyclin B1 and CDK1 in GC-1
359 cells co-cultured with GLY-treated TM4 cells. Given the roles of these proteins in the G2/M-
360 phase transition, this temporal shift may reflect altered coordination between lactate
361 metabolism and cell-cycle progression. The increased proportion of G2/M-phase cells after
362 GLY treatment, along with similar changes after AZD0095 treatment, further supports a
363 functional relationship between lactate availability and cell-cycle regulation. Notably, lactate
364 supplementation attenuated the GLY-associated changes in cell-cycle distribution, providing
365 additional evidence that reduced lactate availability contributes to these alterations. However,
366 the molecular mechanisms underlying lactate-dependent regulation of cell-cycle progression
367 remain unclear.

368 SUMOylation is a reversible post-translational modification involved in mitotic progression,
369 chromosome segregation, DNA damage responses, and cell-cycle control(Dai and Wei
370 2023)(Eifler and Vertegaal 2015b; Vertegaal 2022). SENP1 is a SUMO-specific protease that
371 removes SUMO modifications from target proteins and contributes to the maintenance of
372 SUMOylation homeostasis(Sun et al. 2024). A previous study showed that lactate can inhibit
373 SENP1 through the formation of a lactate–zinc complex at its catalytic site(Liu et al. 2023).

This finding suggests that reduced lactate availability following GLY exposure may weaken the inhibitory effect of lactate on SENP1 by reducing lactate–zinc complex formation at its catalytic site. APC4 is a core component of the APC/C complex and participates in mitotic progression by facilitating the ubiquitin-mediated degradation of cell-cycle regulators(Fehr et al. 2012). Its SUMOylation status may therefore be important for maintaining normal APC/C-dependent cell-cycle regulation(Yatskevich et al. 2021). The present findings suggest that APC4 SUMOylation at K772 and K797 is important for the cellular response to lactate supplementation, particularly the regulation of Cyclin B1 and CDK1 expression and G2/M-phase progression. Reduced lactate availability following GLY treatment of TM4 cells may favor APC4 deSUMOylation through altered SENP1 activity, thereby contributing to G2/M-phase accumulation in GC-1 cells in the co-culture system.

5. Conclusion

This study identifies reduced Sertoli cell-derived lactate availability as a key metabolic factor contributing to GLY-induced male reproductive toxicity. Reduced lactate availability alters SENP1-dependent APC4 SUMOylation, promoting spermatogonial G2/M-phase accumulation and potentially contributing to germ cell loss and impaired spermatogenesis (Fig. 6). These findings reveal a previously unrecognized role for Sertoli cell-derived lactate in regulating spermatogonial cell-cycle progression and provide new insight into the metabolic mechanisms underlying GLY-induced reproductive toxicity.

Declarations

Funding

This work was supported by grants from the National Natural Science Foundation of China (32573442) and Shandong Provincial Natural Science Foundation of China (No. ZR2024MC099).

Ethics approval

All animal experiments in this study were approved by the Committee for the Care and Use of Animals at Shandong Agricultural University (SDAUA-2024-022).

Conflicts of interest

The authors have no competing interests to declare that are relevant to the content of this article.

Data Availability

Data will be made available on request.

References

Bellail AC, Olson JJ, Hao C (2014) SUMO1 modification stabilizes CDK6 protein and drives the cell cycle and glioblastoma progression. Nat Commun 5:4234. https://doi.org/10.1038/ncomms5234

Bøhn T, Millstone E (2019) The Introduction of Thousands of Tonnes of Glyphosate in the food Chain—An Evaluation of Glyphosate Tolerant Soybeans. Foods 8:669. https://doi.org/10.3390/foods8120669

Chang L, Zhang Z, Yang J, et al (2015) Atomic structure of the APC/C and its mechanism of protein ubiquitination. Nature 522:450–454. https://doi.org/10.1038/nature14471

Chen J, Huang Z, Chen Y, et al (2025) Lactate and lactylation in cancer. Signal Transduct Target Ther 10:38. https://doi.org/10.1038/s41392-024-02082-x

Chen X, Liu L, Kang S, et al (2023) The lactate dehydrogenase (LDH) isoenzyme spectrum enables optimally controlling T cell glycolysis and differentiation. Sci Adv 9:eadd9554. https://doi.org/10.1126/sciadv.add9554

Claessens LA, Vertegaal ACO (2024) SUMO proteases: from cellular functions to disease. Trends Cell Biol 34:901–912. https://doi.org/10.1016/j.tcb.2024.01.002

Cluntun AA, Rutter J (2023) The secret life of lactate: A novel cell-cycle regulatory mechanism. Cell Metab 35:730–732. https://doi.org/10.1016/j.cmet.2023.04.006

Dai X, Wei W (2023) Lactate fuels mitosis. Mol Cell 83:1549–1551. https://doi.org/10.1016/j.molcel.2023.04.013

Day JL, Tirard M, Brose N (2024) Deletion of a core APC/C component reveals APC/C function in regulating neuronal USP1 levels and morphology. Front Mol Neurosci 17:1352782. https://doi.org/10.3389/fnmol.2024.1352782

Dong R, Li L, Chang H, et al (2024) Study on the mechanisms of defective spermatogenesis induced by TiO2 NPs based on 3D blood-testis barrier microfluidic chip. Toxicology 507:153888. https://doi.org/10.1016/j.tox.2024.153888

Edenfield RC, Bash JC, Shorey-Kendrick LE, et al (2025) Non-human primates as a translational model for the study of male reproductive health. Nat Rev Urol 22:756–774. https://doi.org/10.1038/s41585-025-01062-2

Eifler K, Cuijpers SAG, Willemstein E, et al (2018) SUMO targets the APC/C to regulate transition from metaphase to anaphase. Nat Commun 9:1119. https://doi.org/10.1038/s41467-018-03486-4

Eifler K, Vertegaal ACO (2015a) SUMOylation-Mediated Regulation of Cell Cycle Progression and

448 Cancer. Trends Biochem Sci 40:779–793. https://doi.org/10.1016/j.tibs.2015.09.006

449 Eifler K, Vertegaal ACO (2015b) SUMOylation-Mediated Regulation of Cell Cycle Progression and
450 Cancer. Trends Biochem Sci 40:779–793. https://doi.org/10.1016/j.tibs.2015.09.006

451 Estermann MA, Sheheen J, Grimm SA, et al (2026a) Glycogen and lactate metabolism in mouse fetal
452 Sertoli cells sustain the germ line. Cell Rep 45:117069.
453 https://doi.org/10.1016/j.celrep.2026.117069

454 Estermann MA, Sheheen J, Grimm SA, et al (2026b) Glycogen and lactate metabolism in mouse fetal
455 Sertoli cells sustain the germ line. Cell Rep 45:117069.
456 https://doi.org/10.1016/j.celrep.2026.117069

457 Fehr AR, Gualberto NC, Savaryn JP, et al (2012) Proteasome-dependent disruption of the E3 ubiquitin
458 ligase anaphase-promoting complex by HCMV protein pUL21a. PLoS Pathog 8:e1002789.
459 https://doi.org/10.1371/journal.ppat.1002789

460 Feng X, Tian J, Han S, et al (2025) Sertoli cells as a hub in testicular development and male
461 reproductive. Front Cell Dev Biol 13:1693878. https://doi.org/10.3389/fcell.2025.1693878

462 Ferreira NGC, da Silva KA, Guimarães ATB, de Oliveira CMR (2023) Hotspots of soil pollution: Possible
463 glyphosate and aminomethylphosphonic acid risks on terrestrial ecosystems and human
464 health. Environ Int 179:108135. https://doi.org/10.1016/j.envint.2023.108135

465 Foy R, Crozier L, Pareri AU, et al (2023) Oncogenic signals prime cancer cells for toxic cell overgrowth
466 during a G1 cell cycle arrest. Mol Cell 83:4047-4061.e6.
467 https://doi.org/10.1016/j.molcel.2023.10.020

468 Griswold MD (2016) Spermatogenesis: The Commitment to Meiosis. Physiol Rev 96:1–17.
469 https://doi.org/10.1152/physrev.00013.2015

470 Gupta VK, Chaudhuri O (2022) Mechanical regulation of cell-cycle progression and division. Trends
471 Cell Biol 32:773–785. https://doi.org/10.1016/j.tcb.2022.03.010

472 Han S, Zhang H, Liu X, et al (2023) Enhanced autophagy reversed aflatoxin B1-induced decrease in
473 lactate secretion of dairy goat Sertoli cells. Ecotoxicol Environ Saf 259:115063.
474 https://doi.org/10.1016/j.ecoenv.2023.115063

475 Jiang Q, Di Q, Shan D, Xu Q (2022) Nonylphenol inhibited HIF-1alpha regulated aerobic glycolysis
476 and induced ROS mediated apoptosis in rat Sertoli cells. Ecotoxicol Environ Saf 241:113822.
477 https://doi.org/10.1016/j.ecoenv.2022.113822

478 Justus CR, Marie MA, Sanderlin EJ, Yang LV (2023) Transwell In Vitro Cell Migration and Invasion
479 Assays. Methods Mol Biol 2644:349–359. https://doi.org/10.1007/978-1-0716-3052-5_22

480 Kroonen JS, Vertegaal ACO (2021) Targeting SUMO Signaling to Wrestle Cancer. Trends Cancer
481 7:496–510. https://doi.org/10.1016/j.trecan.2020.11.009

Li C, Chen W, Cui Y, et al (2024) Essential Regulation of YAP1 in Fate Determinations of Spermatogonial Stem Cells and Male Fertility by Interacting with RAD21 and Targeting NEDD4 in Humans and Mice. Research (Wash D C) 7:0544. https://doi.org/10.34133/research.0544

Li X, Yang Y, Zhang B, et al (2022) Lactate metabolism in human health and disease. Signal Transduct Target Ther 7:305. https://doi.org/10.1038/s41392-022-01151-3

Liu J-B, Li Z-F, Lu L, et al (2022) Glyphosate damages blood-testis barrier via NOX1-triggered oxidative stress in rats: Long-term exposure as a potential risk for male reproductive health. Environ Int 159:107038. https://doi.org/10.1016/j.envint.2021.107038

Liu W, Wang Y, Bozi LHM, et al (2023) Lactate regulates cell cycle by remodelling the anaphase promoting complex. Nature 616:790–797. https://doi.org/10.1038/s41586-023-05939-3

Lombó M, Giommi C, Amoresano A, et al (2025a) The impact of glyphosate at regulatory "safe" levels on reproductive health: cellular and molecular disruptions on male germ line. Environ Int 200:109544. https://doi.org/10.1016/j.envint.2025.109544

Lombó M, Giommi C, Amoresano A, et al (2025b) The impact of glyphosate at regulatory "safe" levels on reproductive health: cellular and molecular disruptions on male germ line. Environ Int 200:109544. https://doi.org/10.1016/j.envint.2025.109544

Maddalon A, Galbiati V, Ferrian M, et al (2025) Immunomodulatory effects of the herbicide glyphosate following occupational exposure. Arch Toxicol 99:4973–4986. https://doi.org/10.1007/s00204-025-04156-3

Maroto M, Torvisco SN, García-Merino C, et al (2025) Mechanisms of Hormonal, Genetic, and Temperature Regulation of Germ Cell Proliferation, Differentiation, and Death During Spermatogenesis. Biomolecules 15:500. https://doi.org/10.3390/biom15040500

Ni F-D, Hao S-L, Yang W-X (2019) Multiple signaling pathways in Sertoli cells: recent findings in spermatogenesis. Cell Death Dis 10:541. https://doi.org/10.1038/s41419-019-1782-z

Pallotti F, Buonacquisto A, Cicolani G, et al (2025) Evolution of the incidence of male fertility disorders over the last decades. Mol Aspects Med 105:101398. https://doi.org/10.1016/j.mam.2025.101398

Rampazzo G, Gazzotti T, Zironi E, Pagliuca G (2023) Glyphosate and Glufosinate Residues in Honey and Other Hive Products. Foods 12:1155. https://doi.org/10.3390/foods12061155

Rato L, Alves MG, Socorro S, et al (2012) Metabolic regulation is important for spermatogenesis. Nat Rev Urol 9:330–338. https://doi.org/10.1038/nrurol.2012.77

Ren Y-L, Chen K, Li Y, et al (2026) Environmental glyphosate exposure compromises sperm quality in mice by impairing acrosome biogenesis via GOLPH3-mediated golgiphagy. J Hazard Mater 503:141086. https://doi.org/10.1016/j.jhazmat.2026.141086

Ren Y-L, Li Z-F, Chen K, et al (2025a) Chronic Dietary Exposure to Environmental Levels of Glyphosate Increases the Risk of Reproductive Dysfunction in Male Mice. Environ Sci Technol 59:15705–15719. https://doi.org/10.1021/acs.est.5c03589

Ren Y-L, Li Z-F, Chen K, et al (2025b) Chronic Dietary Exposure to Environmental Levels of Glyphosate Increases the Risk of Reproductive Dysfunction in Male Mice. Environ Sci Technol 59:15705–15719. https://doi.org/10.1021/acs.est.5c03589

Ren Y-L, Liang Q, Lian C-Y, et al (2024) Melatonin alleviates glyphosate-induced testosterone synthesis inhibition via targeting mitochondrial function in roosters. Environmental Pollution 348:123828. https://doi.org/10.1016/j.envpol.2024.123828

Schwientek M, Rügner H, Haderlein SB, et al (2024) Glyphosate contamination in European rivers not from herbicide application? Water Res 263:122140. https://doi.org/10.1016/j.watres.2024.122140

Souza MCO, Cruz JC, Cesila CA, et al (2023) Recent trends in pesticides in crops: A critical review of the duality of risks-benefits and the Brazilian legislation issue. Environ Res 228:115811. https://doi.org/10.1016/j.envres.2023.115811

Staub C, Johnson L (2018) Review: Spermatogenesis in the bull. Animal 12:s27–s35. https://doi.org/10.1017/S1751731118000435

Sun L, Guo X, Yu M, et al (2024) Human ANP32A/B are SUMOylated and utilized by avian influenza virus NS2 protein to overcome species-specific restriction. Nat Commun 15:10805. https://doi.org/10.1038/s41467-024-55034-y

Vertegaal ACO (2022) Signalling mechanisms and cellular functions of SUMO. Nat Rev Mol Cell Biol 23:715–731. https://doi.org/10.1038/s41580-022-00500-y

Vodermaier HC (2004) APC/C and SCF: controlling each other and the cell cycle. Curr Biol 14:R787-796. https://doi.org/10.1016/j.cub.2004.09.020

Yang X, Yu X, Sun N, et al (2022) Glyphosate-based herbicide causes spermatogenesis disorder and spermatozoa damage of the Chinese mitten crab (Eriocheir sinensis) by affecting testes characteristic enzymes, antioxidant capacities and inducing apoptosis. Toxicol Appl Pharmacol 447:116086. https://doi.org/10.1016/j.taap.2022.116086

Yatskevich S, Kroonen JS, Alfieri C, et al (2021) Molecular mechanisms of APC/C release from spindle assembly checkpoint inhibition by APC/C SUMOylation. Cell Rep 34:108929. https://doi.org/10.1016/j.celrep.2021.108929

Figure Legends

Fig. 1 GLY exposure impairs sperm quality and reduces spermatogonial numbers in mice. (A) Schematic illustration of the animal experimental design. (B) Sperm concentration and motility parameters in the control and GLY-exposed groups (n = 15). (C, D) Representative histopathological images of testicular and epididymal tissues. (E) Testicular and epididymal coefficients (n = 15). (F) Quantification of spermatogonia per seminiferous tubule (n = 6). Data are presented as mean ± SEM. *$p < 0.05$ and **$p < 0.01$.

Fig. 2 GLY-induced changes in Sertoli cell lactate availability accompany altered cell-cycle progression in GC-1 cells. (A) Protein levels and quantitative analysis of Cyclin D1, Cyclin B1, CDK4, CDK6, CDK1, and CDK2 in GC-1 cells at the indicated time points, together with quantitative analysis (n = 3). (B) Representative nuclear images and quantitative analysis of nuclear diameter and nuclear volume in GC-1 cells after co-culture (n = 3). (C) Extracellular lactate levels in TM4 cells at the indicated culture times (n = 6). (D) Extracellular lactate levels in TM4 cells following treatment with GLY at the indicated concentrations (n = 6). (E) Lactate levels in the lower chamber of the Transwell co-culture system at the indicated time points (n = 6). (E) Regression analysis of testicular lactate levels against spermatogonial numbers (n = 6). Data are presented as mean ± SEM; *$p < 0.05$ and **$p < 0.01$ versus the Control group

Fig. 3 Lactate availability regulates cell-cycle progression in GC-1 cells.

(A) Extracellular lactate levels in TM4 cells treated with the lactate transport inhibitor AZD0095 at the indicated concentrations (n = 6). (B) Protein levels and quantitative analysis of Cyclin B1 and CDK1 in GC-1 cells under the indicated treatment conditions (n = 3). (C)

Cell-cycle distribution and quantitative analysis of GC-1 cells under the indicated treatments (n = 3). (D) Representative nuclear images and quantitative analysis of nuclear diameter and nuclear volume under the indicated treatments (n = 3). AZD0095 was used to reduce lactate availability, and sodium chloride (NaCl) served as the control for sodium lactate (LAS) supplementation. Data are presented as mean ± SEM. *$p < 0.05$ and **$p < 0.01$

Fig. 4 SENP1 regulates APC4 SUMOylation and cell-cycle progression in GC-1 cells under reduced lactate availability. (A) Venn analysis of genes associated with germ cell development, male germ cell proliferation, regulation of male germ cell proliferation, and the mitotic cell cycle, together with SENP1 mRNA expression analysis. (B) SENP1 protein levels in testicular tissues and corresponding quantitative analysis (n = 6). (C) SENP1 protein levels and quantitative analysis of GC-1 cells under the indicated lactate-related treatment conditions (n = 3). (D) Protein levels and quantitative analysis of Cyclin B1 and CDK1 in GC-1 cells following SENP1 knockdown under the indicated co-culture conditions (n = 3). (E) Cell-cycle distribution and quantitative analysis of GC-1 cells following SENP1 knockdown under the indicated co-culture conditions (n = 3). (F) Representative nuclear images and quantitative analysis of nuclear diameter and cell volume following SENP1 knockdown under the indicated co-culture conditions (n = 3). Data are presented as mean ± SEM. *$p < 0.05$ and **$p < 0.01$

Fig. 5 APC4 SUMOylation regulates lactate-associated cell-cycle progression in GC-1 cells. (A) Total APC4 protein levels under the indicated co-culture conditions. (B) APC4 SUMO2/3 modification under the indicated co-culture conditions. (C) APC4 SUMO2/3 modification following SENP1 knockdown in GC-1 cells co-cultured with GLY-treated TM4 cells. (D) Schematic representation of the APC4 K772R/K797R double mutant. (E) APC4

SUMO2/3 modification in cells expressing wild-type APC4 or the K772R/K797R mutant. (F) Protein levels and quantitative analysis of Cyclin B1 and CDK1 under the indicated conditions. (G, H) Cell-cycle distribution and quantitative analysis in cells expressing wild-type APC4 or the K772R/K797R mutant. (I, J) Representative nuclear images and quantitative analysis of nuclear diameter and cell volume under the indicated conditions. Data are presented as mean ± SEM. $^{*}p < 0.05$ and $^{**}p < 0.01$

Fig. 6 Reduced Sertoli cell-derived lactate following GLY exposure alters SENP1-dependent APC4 SUMOylation and spermatogonial cell-cycle progression.

A



C57BL/6

Adaptation

1 week

Experiment

24 weeks

Collect testes, epididymis and sperm

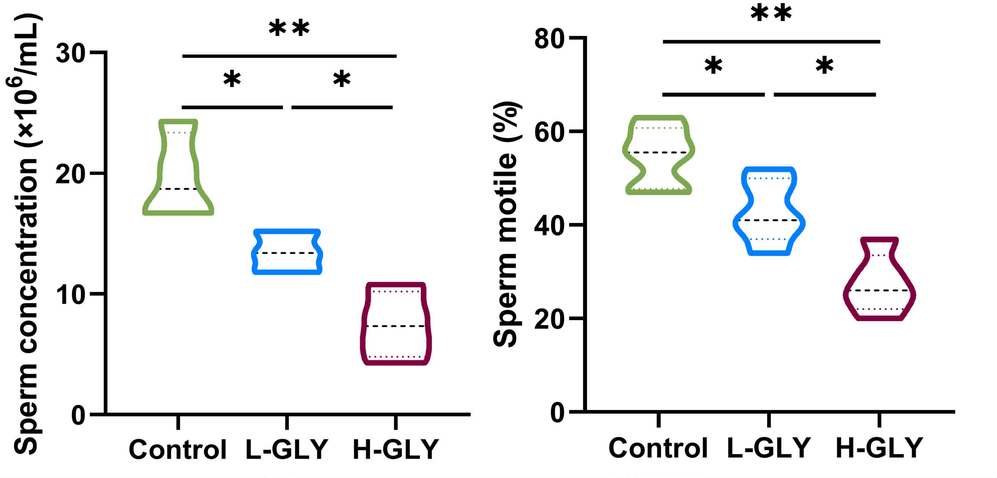
D_{-7} D_0 D_{168}

Control — Normal feed

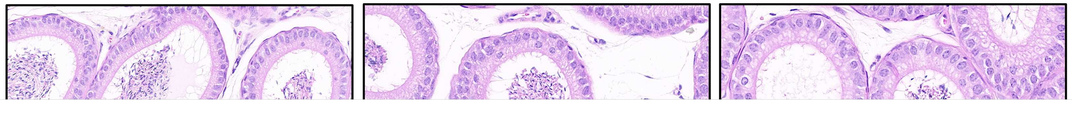
L-GLY — Normal feed — 8.75 mg GLY/kg feed

H-GLY — 87.5 mg GLY/kg feed

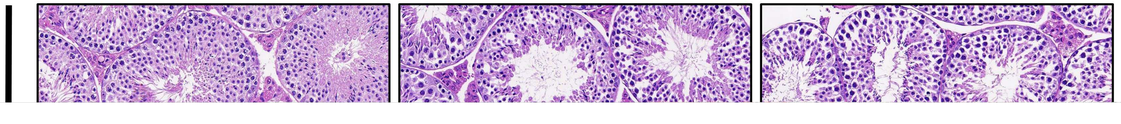
B



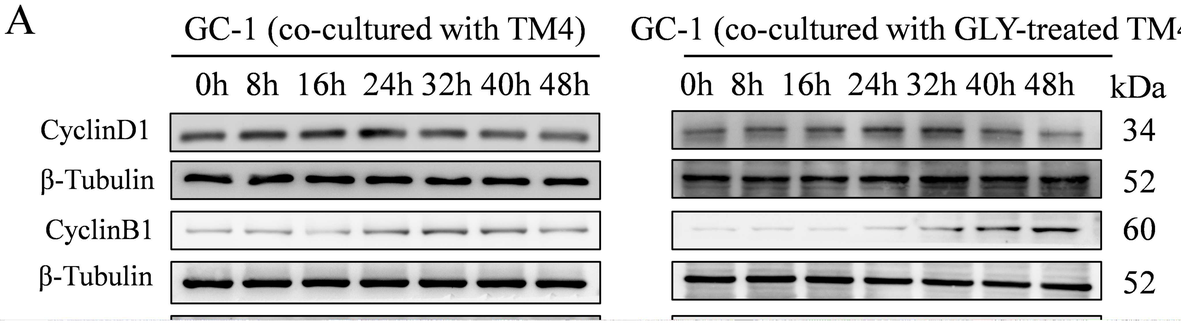
C



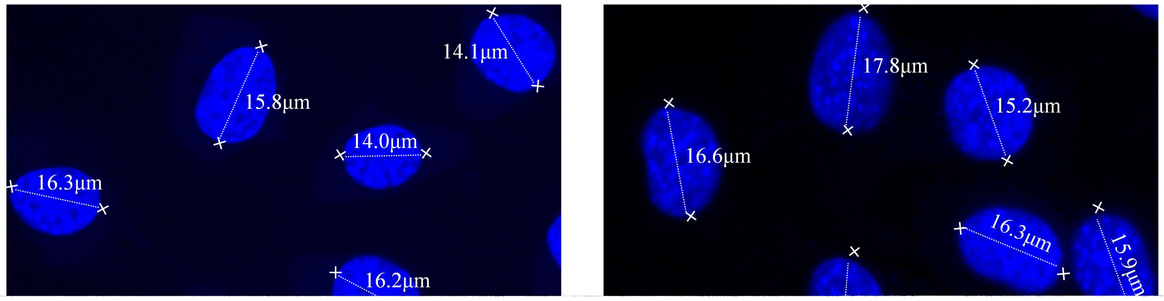
D



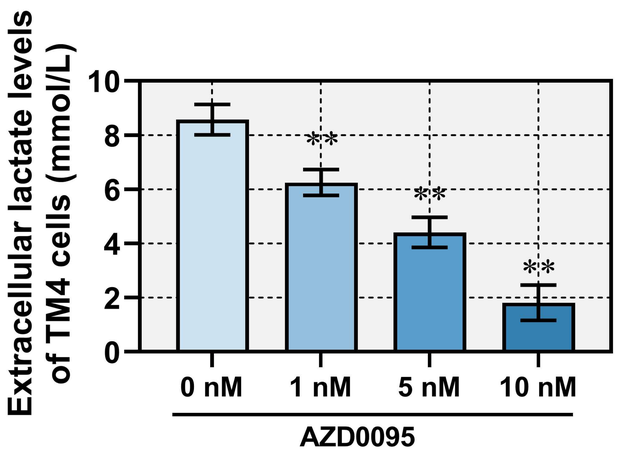
A


GC-1 (co-cultured with TM4)
GC-1 (co-cultured with GLY-treated TM4)
0h 8h 16h 24h 32h 40h 48h
0h 8h 16h 24h 32h 40h 48h
kDa
CyclinD1
β-Tubulin
CyclinB1
β-Tubulin
34
52
60
52

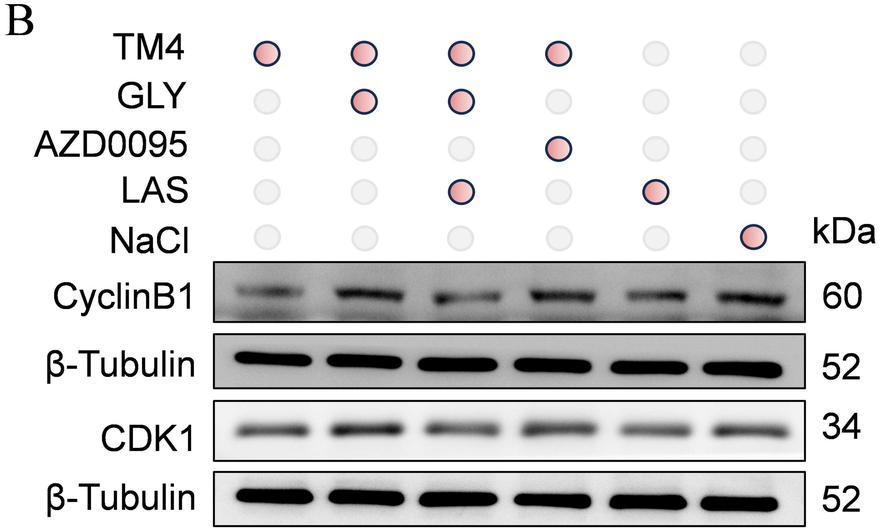
B

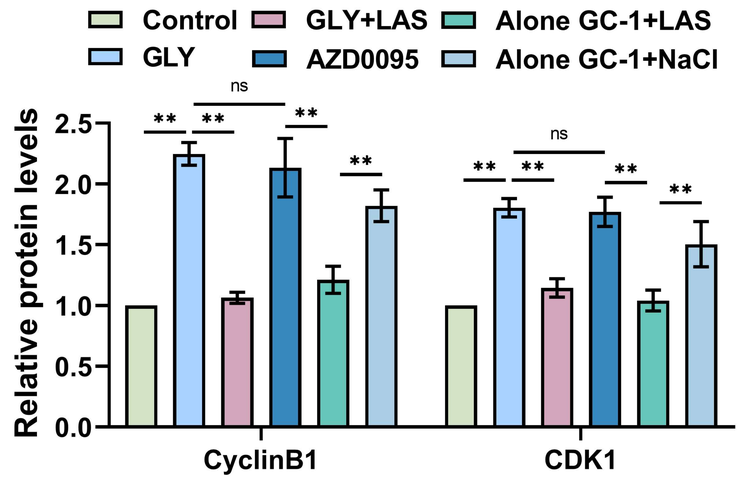

14.1μm
15.8μm
14.0μm
16.3μm
16.2μm
17.8μm
15.2μm
16.6μm
16.3μm
15.9μm

A

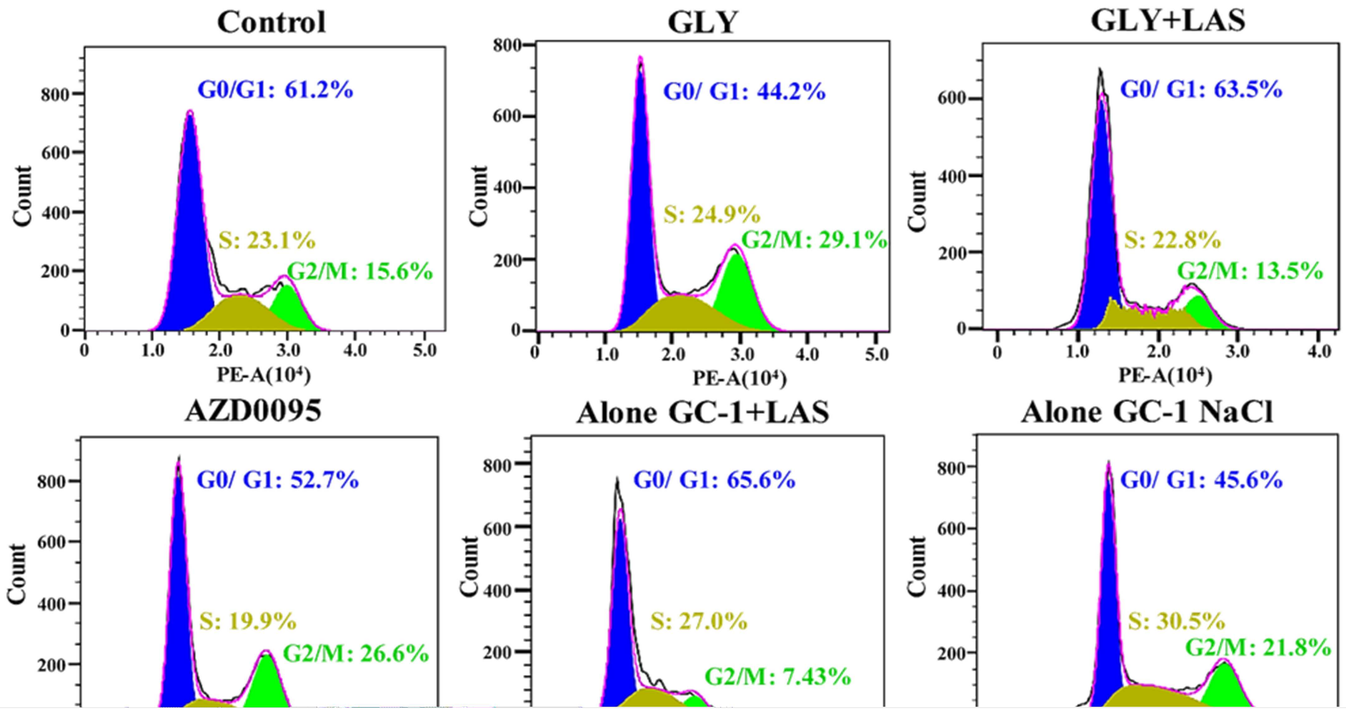

Extracellular lactate levels of TM4 cells (mmol/L)
10
8
6
4
2
0
**
**
**
0 nM
1 nM
5 nM
10 nM
AZD0095

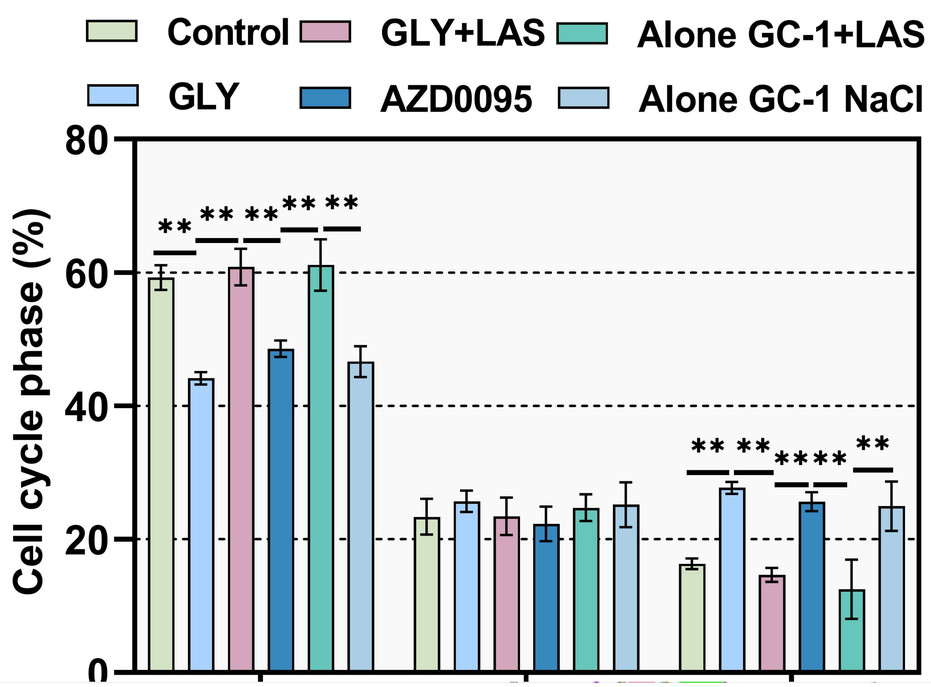
B


TM4
GLY
AZD0095
LAS
NaCl
kDa
CyclinB1
60
β-Tubulin
52
CDK1
34
β-Tubulin
52

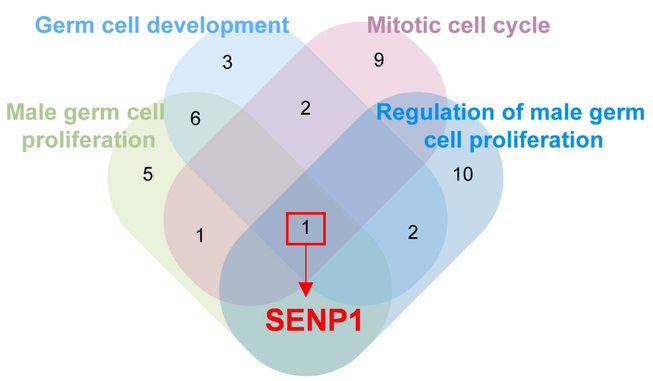

Control
GLY
GLY+LAS
AZD0095
Alone GC-1+LAS
Alone GC-1+NaCl
Relative protein levels
2.5
2.0
1.5
1.0
0.5
0.0
ns
ns
**
CyclinB1
CDK1

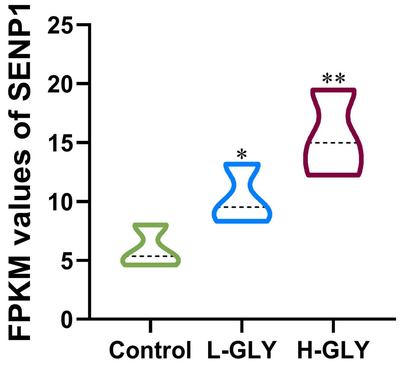
C


Control
G0/G1: 61.2%
S: 23.1%
G2/M: 15.6%
GLY
G0/ G1: 44.2%
S: 24.9%
G2/M: 29.1%
GLY+LAS
G0/ G1: 63.5%
S: 22.8%
G2/M: 13.5%
AZD0095
G0/ G1: 52.7%
S: 19.9%
G2/M: 26.6%
Alone GC-1+LAS
G0/ G1: 65.6%
S: 27.0%
G2/M: 7.43%
Alone GC-1 NaCl
G0/ G1: 45.6%
S: 30.5%
G2/M: 21.8%
Count
PE-A(10⁴)

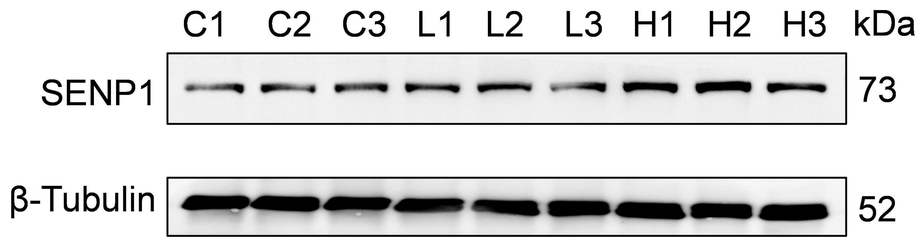

Control
GLY+LAS
Alone GC-1+LAS
GLY
AZD0095
Alone GC-1 NaCl
Cell cycle phase (%)
80
60
40
20
0
**
****
****

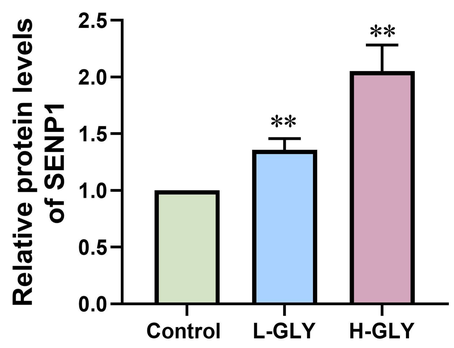
A


Germ cell development
Mitotic cell cycle
Male germ cell proliferation
Regulation of male germ cell proliferation
3
9
6
2
5
10
1
1
2
SENP1

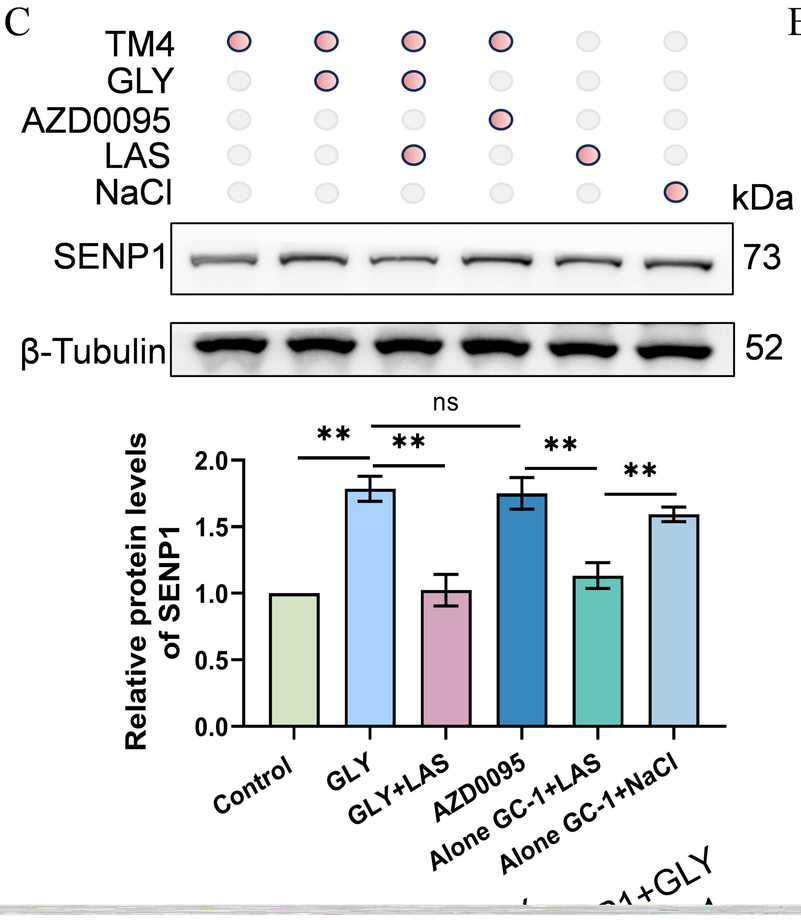

FPKM values of SENP1
Control
L-GLY
H-GLY

B

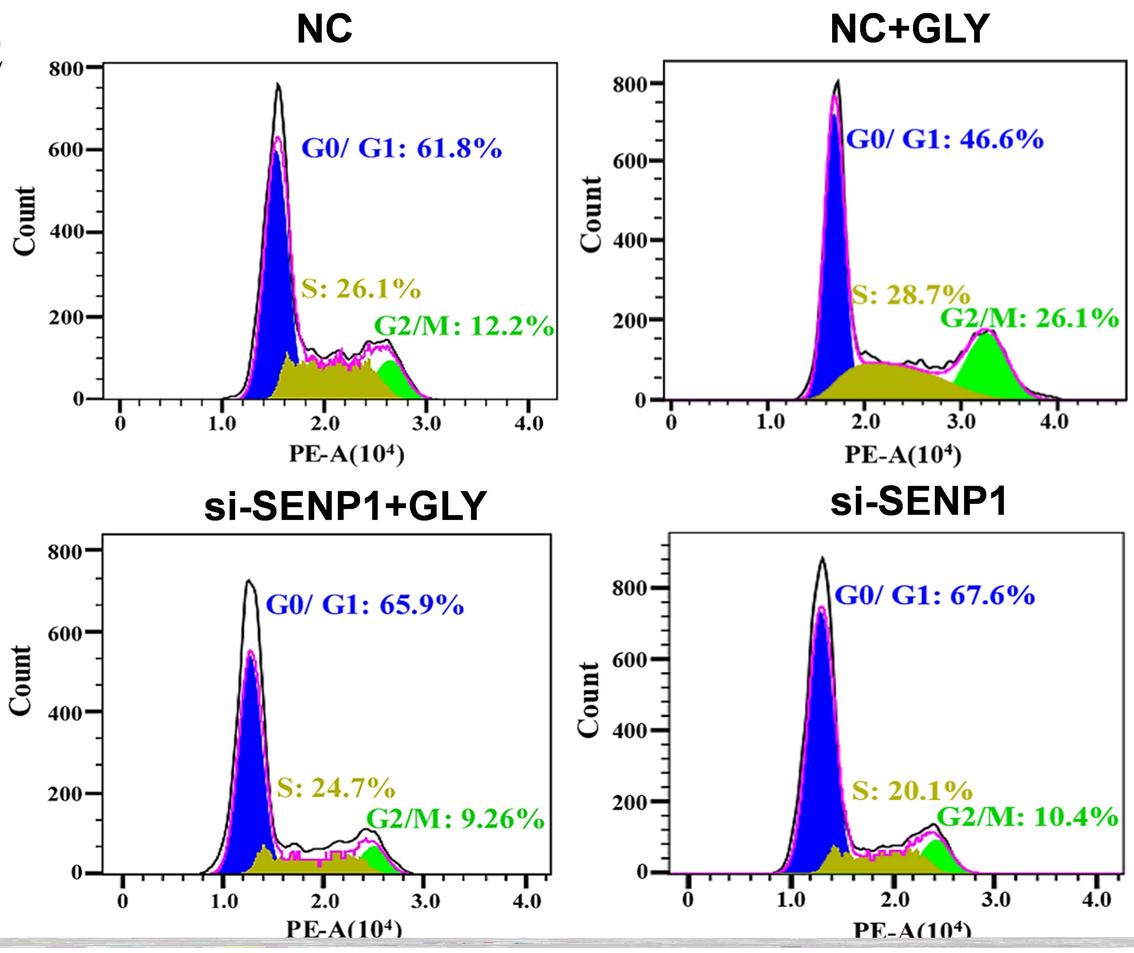

C1 C2 C3 L1 L2 L3 H1 H2 H3 kDa
SENP1
73
β-Tubulin
52

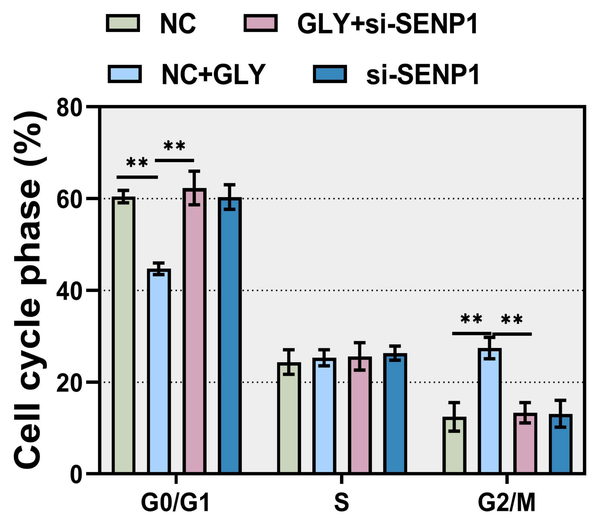

Relative protein levels of SENP1
Control
L-GLY
H-GLY

C

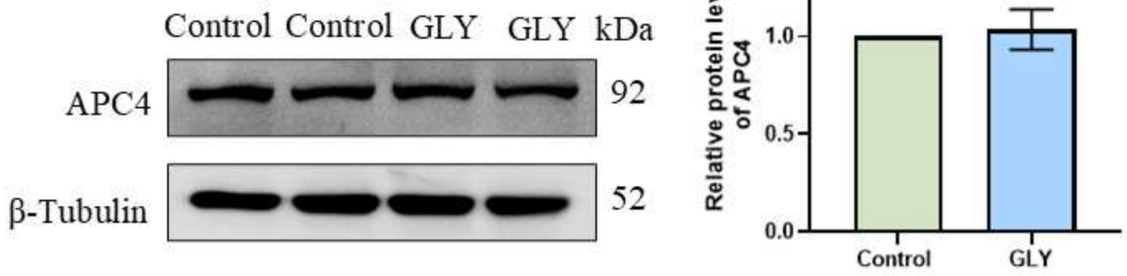

TM4
GLY
AZD0095
LAS
NaCl
kDa
SENP1
73
β-Tubulin
52
ns
Relative protein levels of SENP1
Control
GLY
GLY+LAS
AZD0095
Alone GC-1+LAS
Alone GC-1+NaCl

E

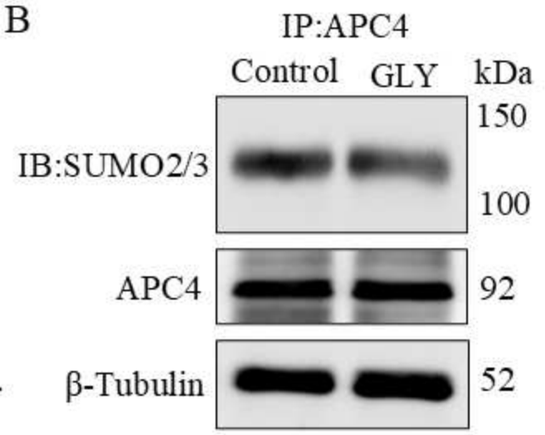

NC
G0/ G1: 61.8%
S: 26.1%
G2/M: 12.2%
NC+GLY
G0/ G1: 46.6%
S: 28.7%
G2/M: 26.1%
si-SENP1+GLY
G0/ G1: 65.9%
S: 24.7%
G2/M: 9.26%
si-SENP1
G0/ G1: 67.6%
S: 20.1%
G2/M: 10.4%
Count
PE-A(10⁴)


NC
GLY+si-SENP1
NC+GLY
si-SENP1
Cell cycle phase (%)
G0/G1
S
G2/M

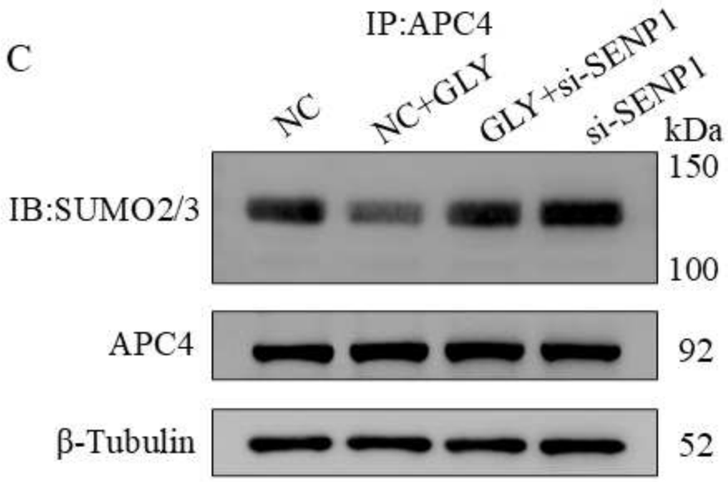
A


Control Control GLY GLY kDa
APC4
92
β-Tubulin
52
Relative protein levels of APC4
1.5
1.0
0.5
0.0
Control
GLY

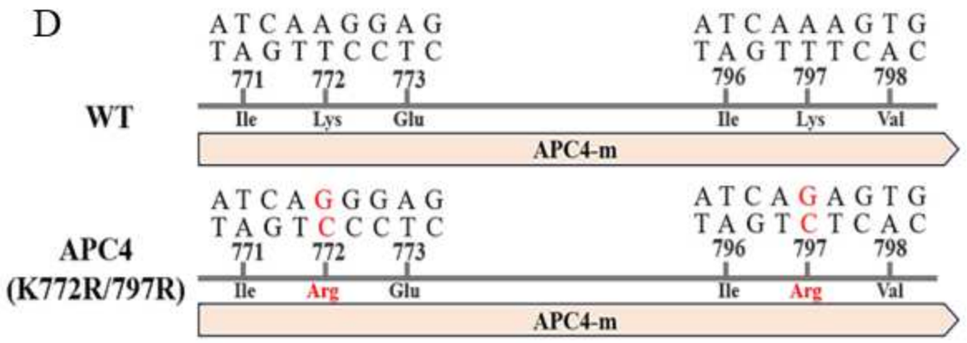
B


IP:APC4
Control GLY kDa
IB:SUMO2/3
150
100
APC4
92
β-Tubulin
52

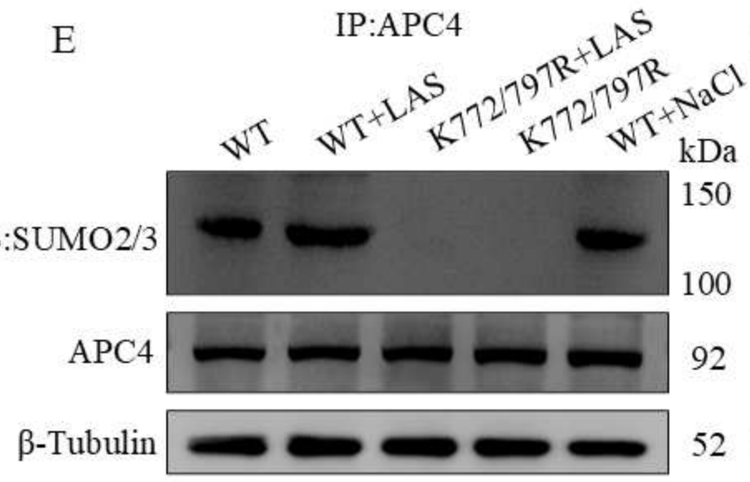
C


IP:APC4
NC
NC+GLY
GLY+si-SENP1
si-SENP1
kDa
IB:SUMO2/3
150
100
APC4
92
β-Tubulin
52

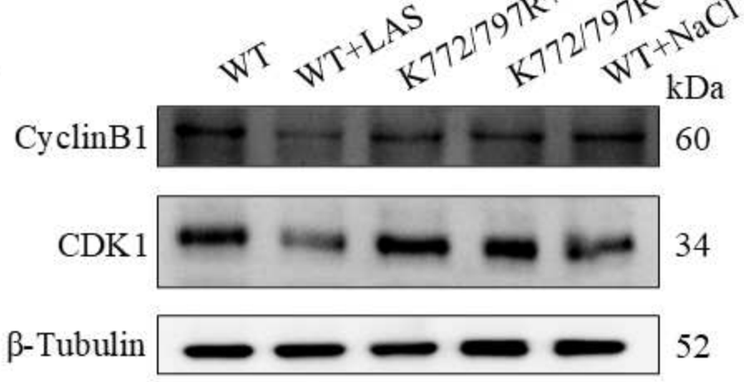
D


WT
A T C A A G G A G
T A G T T C C T C
771 772 773
Ile Lys Glu
A T C A A A G T G
T A G T T T C A C
796 797 798
Ile Lys Val
APC4-m
APC4
(K772R/797R)
A T C A G G A G
T A G T C C T C
771 772 773
Ile Arg Glu
A T C A G A G T G
T A G T C T C A C
796 797 798
Ile Arg Val
APC4-m

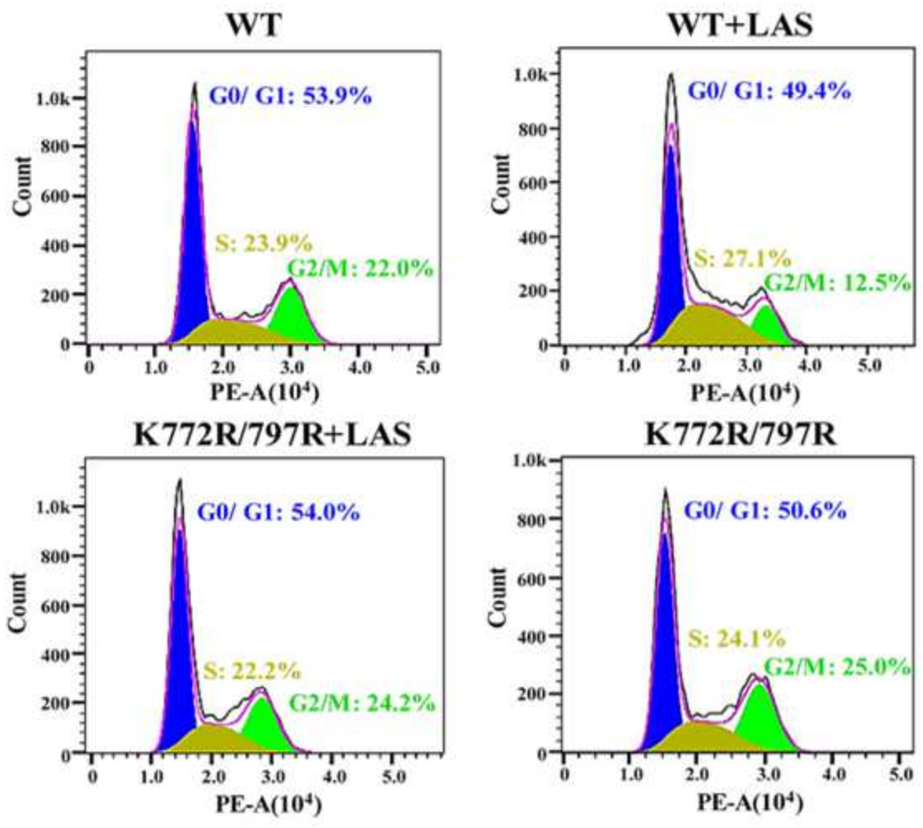
E


IP:APC4
WT
WT+LAS
K772/797R+LAS
K772/797R
WT+NaCl
kDa
IB:SUMO2/3
150
100
APC4
92
β-Tubulin
52

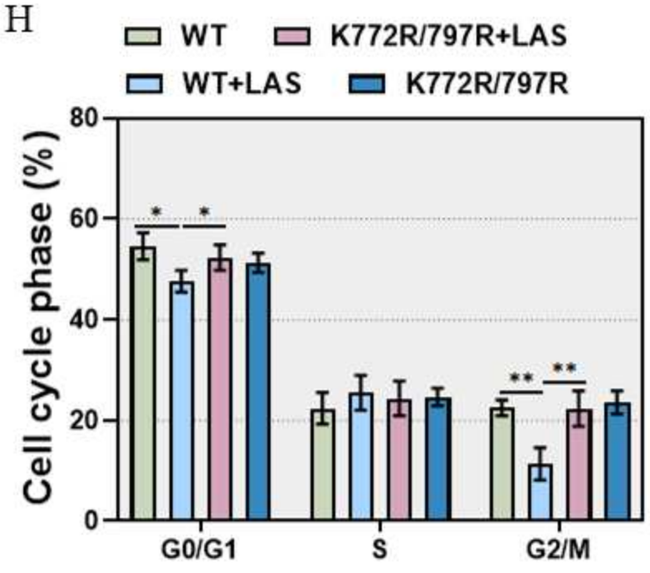
F


WT
WT+LAS
K772/797R+LAS
K772/797R
WT+NaCl
kDa
CyclinB1
60
CDK1
34
β-Tubulin
52

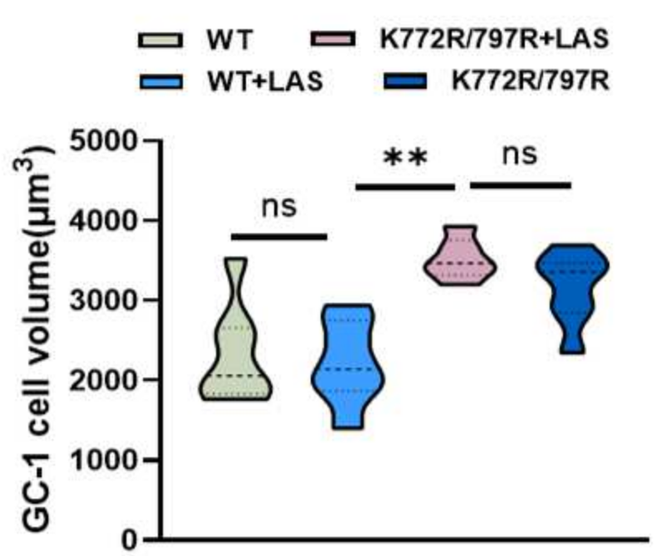
G


WT
G0/ G1: 53.9%
S: 23.9%
G2/M: 22.0%
WT+LAS
G0/ G1: 49.4%
S: 27.1%
G2/M: 12.5%
K772R/797R+LAS
G0/ G1: 54.0%
S: 22.2%
G2/M: 24.2%
K772R/797R
G0/ G1: 50.6%
S: 24.1%
G2/M: 25.0%
Count
PE-A(10⁴)

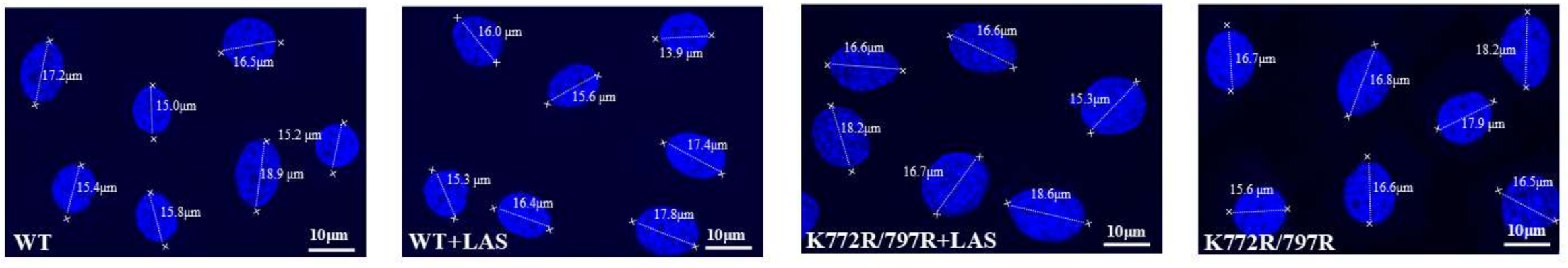
H

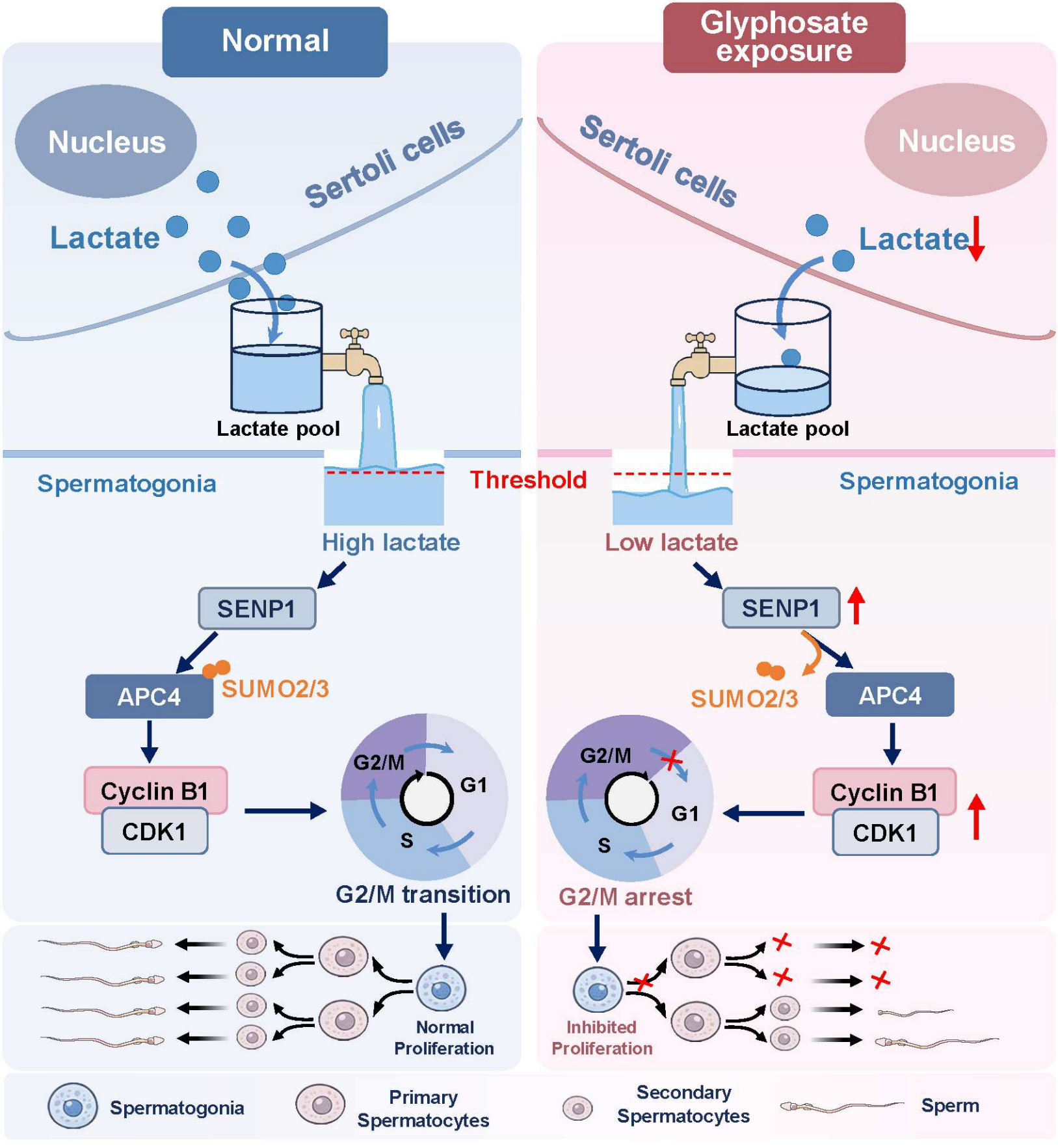

WT
WT+LAS
K772R/797R+LAS
K772R/797R
Cell cycle phase (%)
G0/G1
S
G2/M

J


WT
WT+LAS
K772R/797R+LAS
K772R/797R
GC-1 cell volume(μm³)
ns
**
ns

I


WT
17.2μm
16.5μm
15.0μm
15.2 μm
18.9 μm
15.4μm
15.8μm
10μm
WT+LAS
16.0 μm
13.9 μm
15.6 μm
17.4μm
15.3 μm
16.4μm
17.8μm
10μm
K772R/797R+LAS
16.6μm
16.6μm
15.3μm
18.2μm
16.7μm
18.6μm
10μm
K772R/797R
16.7μm
18.2μm
16.8μm
17.9 μm
15.6 μm
16.6μm
16.5μm
10μm


Normal
Glyphosate exposure
Nucleus
Sertoli cells
Lactate
Lactate pool
Spermatogonia
Threshold
High lactate
Low lactate
SENP1
APC4
SUMO2/3
Cyclin B1
CDK1
G2/M
G1
S
G2/M transition
G2/M arrest
Normal Proliferation
Inhibited Proliferation
Spermatogonia
Primary Spermatocytes
Secondary Spermatocytes
Sperm

Supplementary Files

This is a list of supplementary files associated with this preprint. Click to download.

- SupplementalMaterial.docx